Trop J Nat Prod Res, July 2023; 7(7):3546-3557 **ISSN 2616-0684 (Print)**
ISSN 2616-0692 (Electronic)

Tropical Journal of Natural Product Research

Available online at https://www.tjnpr.org

Original Research Article

β-Amyrin and Benzene-1,2,4-trimethyl from *Euphorbia hirta* L. and *Nauclea latifolia* (Smith) Leaves Induce Dauer Diapause via Antagonist Inhibition of daf-12 Receptor

Olayinka T. Ogunmefun[a,b]*, Oladotun A. Ogunojemite[a], Oluwasegun A. Adedokun[b], Peter T. Olagbemide[a], Ibrahim O. Kehinde[c,d], Mahmoud Soliman[d]

[a]*Department of Biological Sciences, College of Sciences, Afe Babalola University, Ado-Ekiti, Nigeria*
[b]*Department of Pharmacognosy and Natural products, College of Pharmacy, Afe Babalola University,Ado-Ekiti, Nigeria*
[c]*Department of Pharmaceutical and Medicinal Chemistry, College of Pharmacy, Afe Babalola University,Ado-Ekiti, Nigeria*
[d]*Department of Pharmaceutical Science, School of Health Sciences, University of Kwazulu Natal, Durban, South Africa*

ARTICLE INFO

Article history:
Received 21 April 2023
Revised 30 June 2023
Accepted 23 July 2023
Published online 01 August 2023

ABSTRACT

Drug development begins with medicinal plants as valuable materials. *Euphorbia hirta* (EH) and *Nauclea latifolia* (NL) are important medicinal plants having applications in the management of infectious diseases. This research aimed at evaluating EH and NL leaves for their anthelmintic property and establishment of probable dauer diapause effect induced via interaction with daf-12 nuclear receptor in worms using standard procedures. Powdered plant samples were extracted using cold maceration for 72h. Qualitative, quantitative phytochemicals and antioxidants were determined using standard procedures. Metal concentrations were determined using Atomic Absorption Spectrophotometer. Anthelmintic assay was done by observing paralysis and death times of worms. Molecular docking of compounds isolated from plants was done using PyRx-Virtual Screening Tool workspace. SwissADME of the most promising compound was done with online tool. Molecular Dynamics simulation done using UCSF Chimera and graphic processor unit (GPU) version of the PMEMD.CUDA having AMBER package. Different concentrations (10, 30, and 50 mg/mL) of methanol and hexane leaf extracts of EH and NL displayed appreciable anthelmintic activity against *Pheritima pasthuma*, *Taenia solium* and *Fasciola gigantica* in the following order, P. *pasthuma* >*F. gigantica* >*T. solium*. The antagonist effect of Beta amyrin and Benzene-1,2,4-trimethyl on the key Amino acid residues in the binding site of Daf-12 nuclear receptor confer a pronounced dauer diapause effect in EH and NL. *In silico* assay showed Beta-amyrin having promising activity and appreciable stability in the binding site of the target and low bioavailability. This study justifies the reasons behind EH and NL usage as anthelmintic drugs locally

***Keywords*:** Anthelmintic, daf-12 receptor, Dauer diapause, *Euphorbia hirta*, *Nauclea latifolia quadrifida*

Introduction

Helminths are a prevalent class among the various classes of parasitic organisms and infect over a billion people worldwide. They cause problems ranging from malnutrition, physical disabilities, mental retardation, stunted growth and eventually death. Studies have shown that over half of the over 40,000 presumed nematode species are parasitic in nature. [1,2]

Unfortunately, not many treatment regimens exist to combat these parasites or treat host patients to the parasites. The continuous use of anthelmintics for long periods has resulted in resistance over a wide range of time which is now common in livestock infected with parasitic nematodes.[1] As alternative therapies e.g. vaccines are lacking, novel drugs for the treatment of these infections are urgently needed, hence, the choice of medicinal plants,[3,4] or plant based bioactive principle(s) targeting a novel receptor known as nuclear receptor (daf-12) Figure 1A (2–6).

*Corresponding author. E mail: ogunmefunot@abuad.edu.ng
yinkatayo_08@yahoo.com
Tel: +2348038640115

Citation: Ogunmefun OT, Ogunojemite OA, Adedokun OA, Olagbemide PT, Kehinde IO, Soliman M. *β*-Amyrin and Benzene-1,2,4-trimethyl from *Euphorbia hirta* L. and *Nauclea latifolia* (Smith) Leaves Induce Dauer Diapause via Antagonist Inhibition of daf-12 Receptor. Trop J Nat Prod Res. 2023; 7(7):3546-3557 http://www.doi.org/10.26538/tjnpr/v7i7.38

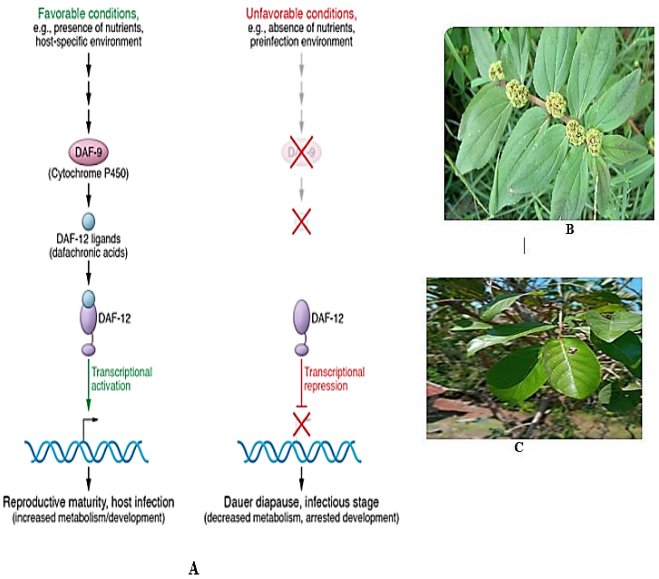

Figure 1: A - Role of daf-12 in reproduction and development of parasite in host organism, B - *Euphorbia hirta***,** C - *Nauclea latifolia* in their natural habitats

Ligand-gated transcription factors regulating various biological processes such as metabolism, development and reproduction are known as nuclear receptors.[6]
Nuclear receptors are now attractive targets for developing orally available small-molecule drugs because of their ligands' lipophilic nature and the expression of multiple genes being modulated by them within the same pathway.[6,10] A novel therapeutic strategy different from current anthelmintics, that focus on tubulins (Benzimidazoles), ion channels (Ivermectin and Diethylcarbamazine), or symbiotic bacteria of parasites (Doxycycline) could be developed by targeting nuclear receptors,5 Figure 1A.8
In addition, there are numerous medicinal plants with ethnomedicinal usage in the treatment of helminths, most important of them are Euphorbia hirta and Nuclea latifolia.[7,8]
Euphorbia hirta (Family Euphorbiaceae) (Figure 1B) is an anthropogenic herb that is commonly found in open waste spaces widely throughout West Tropical Africa and it is well known for its antibiotics, diuretic and purgative properties.[11,13,14]
Nauclea latifolia (Family Rubiaceae) (Figure 1C), a straggling shrub or small tree, native to Tropical Africa and Asia is used in treating diarrhoea, fever and as an anti-parasitic drug.12 However, this study was therefore designed to evaluate the anthelmintic properties of E. hirta and N. latifolia leaf extracts and to determine the mechanism of action of the bioactive principle(s) from both plants on nuclear receptor (daf-12).

Materials and Methods

Collection of plant materials
Euphorbia hirta fresh leaves were collected from Ikere-Ekiti market while the fresh leaves of Nauclea latifolia were collected in Ado-Ekiti (Global Positioning System (GPS) location of 7° 37' 15.9996" N and 5° 13' 17.0004" E), both in Ekiti State in June/July, 2020. The plants (leaves) were identified and authenticated by a plant taxonomist at the herbarium section of the Department of Plant Science and Biotechnology, Ekiti State University, Ado-Ekiti, Nigeria and voucher specimens of the two plants were deposited at the herbarium, with Euphorbia hirta and Nauclea latifolia having herbarium numbers UHAE 2020061 and UHAE 2020078, respectively.

Preparation of plant extracts
The two plant samples were air dried at room temperature (about 20°C) for 14 days. The dried leaves of the two plants were powdered separately and stored in air tight bottles until needed. Hundred (100) grams of each plant powdered samples was soaked in a container with 1000 mL of methanol and hexane separately. The samples were shaken vigorously and kept for 72h using cold maceration method, this was further concentrated in vacuo employing a rotary evaporator (Serial Number: R000100958, Bibby Scientific Limited, Stone, Staffordshire, ST15 OSA, UK) at 45oC. Well labelled airtight bottles were used in storing the resulting extracts and kept in the refrigerator at 5oC till further use.[9,10]

Phytochemicals Qualitative procedures
Preliminary phytochemical screening was done following standardized procedures as described.[9, 10]

Phytochemical Quantitative Procedures
Determination of Total Phenolic Content
Five Hundred microliter (500 µL) of extract was placed into a test tube with Five Hundred microliter (500 µL) Folin-Ciocalteu solution with the addition of one milliliter (1 mL) Sodium carbonate solution and eight milliliter (8 mL) distilled water; the samples remained at room temperature for 30 minutes. The spectrophotometer at 760 nm wavelength was used and the total phenol content was expressed as milligrams of Tannic acid equivalents per gram of extract (mg TAE/g).[11]

Determination of Tannins Content
Five hundred (500 mg) milligram of casein was transferred into a 25 mL Erlenmeyer flask after which 5 mL each of the extracts and distilled water were added. After two hours i.e. time required for the tannins to be complexed to the total protein, the filtered extracts were poured separately into a 10 mL volumetric flask and volume adjusted with distilled water. Five Hundred microliter (500 µL) extract was placed into a test tube, with the addition of Folin-Ciocalteu solution (500 µL), Sodium carbonate solution (1 mL) and distilled water (8 mL) with the samples remaining at room temperature for 30 minutes. The spectrophotometer (Spectrumlab 752s, Gallenkomp, England) was read at 760 nm wavelength and total phenol content expressed as milligrams of tannic acid equivalents per gram of extract (mg TAE/g).*12,13*

Determination of Flavonoids Content
Leaf extracts (500 µL) each was transferred into separate test tubes with the addition of Acetic acid solution (500 µL), Pyridine solution (2 mL), Aluminium chloride solution (1 mL) and 80% Methanol (6 mL); while samples were kept for 30 minutes at room temperature and the absorbance read at 420 nm. The flavonoid content was expressed as milligrams of quercetin equivalents per gram of extract (mg QE/g).14-16

Determination of alkaloids content
Each extract (2 g) of the leaves of E. hirta and N. latifolia were placed in a 250 mL beaker;10% Acetic acid (80 mL) in Ethanol was added, covered and allowed to stand for 4 hours after which it was filtered and concentrated on a water bath (HH-S Water Baths, China) to about a quarter of the initial volume. Drops of concentrated Ammonium were added to the extracts until precipitation was completely achieved. The solution was allowed to settle with the precipitate collected, washed with dilute Ammonium hydroxide and filtered. The residue was dried and weighed and that is the alkaloid.[17]

Determination of saponins content
Two grams (2 g) of each powdered sample were weighed separately into conical flasks, with 20 mL of 20% aqueous Ethanol added. It was then heated over water bath for 4 hours while stirring continuously at 55°C. This mixture was filtered and the residue re-extracted with another 200 mL of 20% Ethanol. These extracts were reduced to 40 mL separately over water bath at about 90°C. Twenty millilitres (20 mL) of Diethyl ether was added to the concentrates inside a 250 mL separator funnel and shaken vigorously. The aqueous layer was recovered while the ether layer was discarded. There purification process was repeated with an addition of 60 mL n-butanol. Ten millilitres (10 mL) of 5% aqueous Sodium chloride was used in washing the combined n-butanol extracts twice; while the remaining solution was heated over the water bath. After evaporation, the samples were dried in the oven (DHG - 9035A, Gallenkomp, England) to a constant weight to give the saponins which was then calculated.[18,19]

Saponins contents= (W1-W2)/W3

Where,
W1 = Weight of conical flasks + sample before drying
W2 = Weight of conical flasks + sample after drying
W3 = Weight of sample

Determination of Anthraquinones Content
Into a 100 mL volumetric flask was added 10mL of the sample which was adjusted to the required volume with solvent and analyzed at 325 nm wavelength using UV-Vis spectrophotometer (Spectrumlab 752s, Gallenkomp, England). Determination of the concentration was by checking the dilution factor of each sample in comparison to the standard anthraquinone solution.[10]

Determination of Steroids Content
To each of the test extracts (1 mL) in volumetric flasks (100 mL) was added Sulphuric acid (4N, 2 mL) and Iron (lll) chloride (0.5% w/v, 2 mL), after which Potassium hexacyanoferrate (lll) solution (0.5% w/v, 0.5 mL) was added. The mixture was heated in a water bath for 30 minutes with temperature at 70±2o C, shaken occasionally and diluted to reach the mark assigned in the volumetric flask with distilled water. Absorbance against the reagent blank was measured at 780nm.[14]

Determination of Terpenoids Content
Ten millilitres (10mL) Petroleum ether was used to partition one gram (1 g) of each extract in a separating funnel. The ether extract in pre-weighed glass vials was separated and waited for until completely dried. The yield (%) of total terpenoids contents was measured by the formula below after Petroleum ether was evaporated.[20]

Yield (%) of total terpenoids= (W1-W2)/W1 X 100

Where,
W1 = Weight of Ether extract before drying
W2 = Weight of Ether extract after drying

Determination of Glycosides Content
Each sample (10 g) was treated with Lead acetate solution for tannins, proteins, colouring matter and other non-glycoside parts to be precipitated. Filtration of the precipitate formed was done and Hydrogen sulphide gas was made to pass through the filtrate to precipitate excess Lead as Lead sulphides, which was removed by filtration. Evaporation of the filtrate to dryness was done on a water bath (HH-S Water Baths, China) and the residue dried, collected and weighed to get the total glycoside content.[20]

Determination of Reducing Sugar
Each sample (100 mg) was weighed and the sugar extracted with hot Ethanol (80%). The supernatant after collection was evaporated at 80OC on a water bath. Distilled water (10 mL) was added to dissolve the sugars while 0.1mL was separated into test tubes using a pipette.
Preparation of working standard (0.2, 0.4, 0.6 and 0.8 mL) into series of test tubes was done. Both samples were made up to 2 mL each with distilled water in standard tubes. Two milliliters (2 mL) of distilled water was separated as blank and to each standard tube was added 1mL of alkaline Copper tartrate reagent. The two standard tubes were left for 10 minutes in a water bath. It was allowed to cool down and Arsenomolybolic acid (1 mL) was added to each of the test tubes and made up with distilled water to 10 mL. The absorbance was read at 620nm when the colour turned blue at the end of 10 minutes. The quantity of reducing sugars present was calculated from the graph drawn.[10,21]

Metal/Mineral Analysis
Spectrophotometry was the method used for analysing metal concentration using Atomic Absorption Spectrophotometer (AAS) Buck Scientific model 211 VGP employing the calibration plot method. The three processes involved were; preparation of standard, calibration of equipment and analysis of sample. The instrument was auto-zeroed using the blank (distilled water) for each element. The standard from the lowest to the highest concentrations was then aspirated into the flame. The graph of absorbance against concentration was plotted after the corresponding absorbance was obtained by the instrument. Analysis of the samples was done with the concentration of the metals present expressed in parts per million (ppm) having extrapolated from the standard curve.[22]

Radical scavenging activity of extracts using Diphenyl-2-Picryl-Hydrazyl (DPPH) method
The free radical scavenging capacity of the plant extracts against 1, 1 – Diphenyl – 2 – picryl-hydrazyl (DPPH) free radical was measured using the modified method;23 DPPH (0.1 mM) was added to different concentrations of each sample. Vitamin C (positive control) was also used as standard drug at same concentration range (20 - 100 µg/mL), followed by incubation in an incubator (Model NO. 9052A, Gallenlomp, England) for one hour in the dark and optical density (OD) of the samples was measured at 517 nm against a blank and percentage (%) inhibition was calculated from the absorbance values.

% DPPH inhibition= (A-B)/A X 100

Where A is the absorbance of pure DPPH in oxidized form while B is the absorbance of sample taken after 60 minutes of reaction with DPPH.[11]

Determination of Ferric Reducing Antioxidant Property (FRAP)
The reducing property of the extracts was determined by.11 Each extract of about 0.25mL was mixed with 0.25 mL of 200 mM of Sodium phosphate buffer (pH 6.6) and 0.25mL of 1% Potassium Ferrocyanide (KFC). Incubation of the mixture was done for 20 minutes at 50oC, then 0.25mL of 10% TCA was added and centrifuged at 2000 rpm for 10minutes; the supernatant (1mL) was mixed with 1mL of distilled water and 0.2 mL of 1% Ferric chloride and the absorbance was measured at 700 nm.[1]

Anthelmintic assay
Collection and authentication of worms
Taenia solium (Tapeworm) 2.2–2.6 g and Fasciola gigantica (Liverfluke) 0.04-0.08 g were obtained from a slaughtered cow at the Irasa Abattoir in Ado-Ekiti metropolis (M7W4+RG5, Ado-Iworoko road, 362103, Ilokun, Ekiti) by exactly 7:00 am in the morning. Pheritima pasthuma (Earthworm, 0.09–0.8 g) were collected from a waterlogged area of Ekiti State University Farm with GPS location of N 7° 42' 50.8032", E 5° 15' 36.1332 at exactly 8:30am. The worms were identified at the Zoology and Environmental Science Department of Ekiti State University, Ado-Ekiti, Nigeria.

Bioassay
A worm was placed in each petri dish containing the extracts of E.hirta and N.latifolia using three different concentrations (10, 30 and 50 mg/mL in distilled water) respectively. This was carried out in duplicates for each worm type. The average (mean) times for paralyses (P, in minutes) were taken when no movement was observed, except when there was vigorous shaking of the worms. Death times of worms (D, in minutes) were recorded after no movement of worms either on their own or when vigorously shaken was ascertained. Antepar (10 mg/mL) was used as a standard drug i.e. reference compound, while distilled water served as the control.[24-27]
Molecular docking of the compounds isolated from E. hirta and N. latifolia on nuclear receptor daf-12

System Preparation
Retrieval and Preparation of Protein
The protein target preparation was accomplished through the 3D crystalline structure of worm nuclear receptor (PDB ID: 3UP3, Resolution: 1.25 Å) bound with its co-crystallized antagonists (25s)-cholestenoic acid (CID: 10001991), obtained from Protein Data Bank (PDB). The protein crystal structure was expressed from Ancylostom aceylanicum, Homosapiens and was prepared before docking using UCSF Chimera 1.14 tool via removal of ions, water, and bound ligands which are non-standard residues. The structural minimization of the proteins was carried out at 200 steepest descent steps, 0.02 steepest descent steps size (Ă), ten conjugate gradient steps, and 0.02 conjugate gradient steps size (Ă) 10 update intervals using the structure editing wizard. There was removal of solvents, addition of Hydrogen bonds, allocation of charges through the Gasteiger force field and protonation state through setting of Histidine. Selenomethionine (MSE) present was changed to Methionine (MET), Bromo-UMP (5BU) to UMP (U), MethylselenyldUMP (UMS) to UMP (U) and Methylsulfonyl-dCMP (CSL) to CMP (C).[28]

Ligand Selection and Preparation
This study made use of ligands that are 3D chemical structures of compounds isolated from E. hirta and N. latifolia. The structure data file (SDF) format of the compounds was retrieved from the PubChem database; PDB coordinates of all compounds were optimized by the UCSF Chimera tool, and charges were computed and added to the ligands through ANTECHAMBER.[29]

Molecular Docking
The prepared proteins and ligands were uploaded to the PyRx-Virtual Screening Tool workspace. A blind docking was initially carried out where the ligands were docked to the whole surface of the protein, followed by a site-specific docking to the co-factor and substrate binding pocket as identified in a previous study.30,31 Using the Autodock Vina of PyRx software, the grid box was set for docking

based on the dimensions of the protein structure; each ligand-receptor binding.[30, 31]

Molecular interaction
Bovia Discovery 2020 Client was used to carry out molecular interaction (visualization) between the pharmacophore of the ligands and amino acid residues in the pocket of the indicated target.[32]

Swiss ADME of most promising compound
The online tool, namely: SwissADME (www.swissdock.ch) was used for detailed in silico physicochemical and pharmacokinetics studies of the compounds.[33]

Molecular Dynamics (MD)
The ligands and the receptor were prepared for the Molecular Dynamics simulation using UCSF Chimera. The MD simulation enquiries were done for the protein and complexes with the most potent compound (Apo+ligand) and cholestenoic acid (Apo+control) with the aids of the graphic processor unit (GPU) version of the PMEMD.CUDA engine equipped with the AMBER package, FF18SB variant of the AMBER forcefield used in defining the protein. The stability of the complexes was estimated by computing MD simulations studies. The GENERAL AMBER Force field (GAFF) and the restrained electrostatic potential (RESP) methods aids in the addition of partial charges to the ligands and were improved using ANTECHAMBER. Neutralization and solvation were done with the assistance of LEAP module in AMBER 18 which helps in adding charges; H+, Na+ and Cl counter ions to the unbound protein and ligand-bound systems. Also, all-atoms explicit solvation was carried out in an orthorhombic TIP3P box of water molecules sized 10 Å. The initial minimization (2500 steps) and complete minimization (5000 steps) were performed through a conjugate algorithm. Heating of the systems from 0 to 300 K were conducted for 50 ps. The total length of the simulation time was 200 ns with a time scale of 2 fs using a Langevin thermostat, at 300 K, and 1 bar constant pressure. The coordinates of the Apo-protein, Apo+control and Apo+ligand complexes were saved every 1 ps. All trajectories were studied for RMSD, RMSF and radius of gyration using CPTRAJ and PTRAJ module in AMBER 18/GPU. The investigates of post-MD structures and visualization were observed by using the graphical user interface of UCSF Chimera and Discovery studio 2021 client to enable the study of the mechanism of binding of the ligand-bound systems and MicroCAl Origin 6.0 software for data analysis was used to plot the data.[34-36]

Statistical analysis
Microsoft excel and Graph pad prism 7 (version 8) were used for the analyses of all data collected from the entire study. Presentation of the pertinent points was done using relevant tables, charts, and descriptive statistics. The mean ± SEM of three replicates was used to express data for the in vitro model. One Way Analysis of Variance (ANOVA) complemented with Krystal-Wallis's test was used to statistically analyze data.

Results and Discussion

Result of qualitative phytochemical screening
Different classes of phytochemicals (secondary metabolites) were observed in the two plants and these classes of compounds include: alkaloids, phenols tannins, saponins, flavonoids, steroids, anthraquinones, cardiac glycosides, terpenoids and reduced sugar compounds (Table 1).

Quantitative phytochemistry of plant samples
According to the quantitative analysis shown in Table 2, Euphorbia hirta was observed to having high level of alkaloids of about 1243 mg/100 g of crude extracts, followed by saponins (787 mg/100g) with low amount of reduced sugar (0.4 mg/100 g). Nauclea latifolia was observed with high level of flavonoids (746 mg/100 g) and low level of reduced sugar of about 1 mg/100 g, which is higher than that of Euphorbia hirta.

Results of mineral analysis of plant samples
Euphorbia hirta and Nauclea latifolia exhibited high level of Potassium of about 2896 ppm and 314.8 ppm respectively and low amounts of Lead of 0.007 ppm and 0.002 ppm as shown in the Table 3.

Table 1: Preliminary phytochemical screening of *E. hirta* and *N. latifolia*

Phytochemicals	***Euphorbia hirta***	***Nauclea latifolia***
Alkaloids	+	+
Phenolics	+	+
Tannins	+	+
Saponins	+	+
Flavonoids	+	+
Steroids	+	-
Anthraquinones	+	+
Cardiac glycosides	+	-
Terpenoids	+	+
Reducing sugar	-	-

Keys: + = Present; - = Absent

Table 2: Amounts of Phytochemicals in *Euphorbia hirta* and *Nauclea latifolia* leaves

Phytochemicals (mg/100g)	***Euphorbia hirta***	***Nauclea latifolia***
Alkaloids	1243	388
Phenols (GAE/g)	46	68
Tannins	978	532
Saponins	787	532
Flavonoids	528	746
Steroids	182	108
Anthraquinones	113	87
Cardiac glycocides	35	13
Terpenoids	168	377
Reducing sugar	0.4	1

Table 3: Mineral Analysis of *Euphorbia hirta* and *Nauclea latifolia* leaf extracts

Parameters (ppm)	***Euphorbia hirta***	***Nauclea latifolia***
Na	161.55	108.35
Ca	140.60	92.25
K	2896.00	314.80
Mg	7.203	41.076
Fe	13.002	0.396
Mn	2.690	0.446
Pb	0.007	0.002
Zn	9.420	6.18
Cu	0.530	0.742
Cr	0.100	0.031
Se	0.108	0.079

Antioxidant activity of the plant samples

The effective concentration required for radical scavenging of Euphorbia hirta (EH) and Nauclea latifolia (NL) is 1.13 µg/mL and 1.63 µg/mL respectively, however from the result it was noted that the effective concentration of EH for DPPH is better than that of NL. Also, Ferric reducing antioxidant power (FRAP) assay concentration of EH was observed to be better when compared to NL. However, the Oxygen Radical Absorbance Capacity (ORAC) percentage inhibition showed that NL inhibited a larger amount of Peroxyl radical induced oxidation compared to EH as shown in Table 4.

Anthelmintic studies of the plant extracts

A decrease in time of paralysis (P) and death (D) was observed generally for the methanol extract of the two plants examined at different concentrations in a concentration dependent pattern. However, methanol extract of E. hirta at 50 mg/mL showed more potent activity against P. pasthuma with a time of paralysis and death of 7.00 ± 0.20 and 41.00 ± 0.30 respectively relative to the negative control (distilled water) at $p<0.05$ among the parasites examined as shown in Table 5. It is noteworthy to state that all the concentrations of methanol extract of EH had a significant effect on the time of paralysis and death of T. solium, P. pasthuma and F. gigantica relative to the negative control $p<0.05$.

However, significant observation was noted, when an increase in the concentration of NL (10 – 50 mg/mL) influenced a decrease in both times of paralysis and death in P. pasthuma relative to other organisms. Nauclea latifolia at 10 and 50 mg/mL produced 16.00 ± 0.50 (P); 55.00 ± 0.20 (D) and 6.00 ± 0.10 (P); 30.00 ± 0.20 (D) respectively which is more potent than 18.00 ±0.20 (P); 52.00 ± 0.1 (D) observed with 10 mg/mL Antepar (positive control) and distilled water (negative control) at $p< 0.05$.

A similar pattern of results observed above (Table 5) was noted for n-hexane especially concentration increase (10 – 50 mg/mL) induced a significant reduction in the time of paralysis (P) and death of P. pasthuma relative to other worms (10 mg/mL – 19.00 ± 0.30 (P); 62.00 ± 0.10 (D) while 50 mg/mL – 10.00 ± 0.40 (P); 43.00 ± 0.20 (D) relative to 10 mg/mL antepar (positive control) and distilled water (negative control) at $p<0.05$. In addition, the hexane extract of NL also exhibits a significant and promising effect on T. solium and P. pasthuma in a concentration-dependent manner with 50 mg/mL of the sample regarded as the most effective for the two parasites $p<0.05$ (13.00 ± 0.10 (P), 40.00 ± 0.50 (D) and 8.00 ± 0.30 (P); 32.02±0.20 (D) for T. solium and P. pasthuma respectively as shown in Table 6.

Molecular docking of compounds isolated from E. hirta (EH) with Daf-12 receptor

Compounds isolated from EH were subjected to molecular docking with daf-12 nuclear receptor present in all the worms examined, this resulted in beta-amyrin having the lowest binding affinity of -11.90 relative to -12.5 observed with (25s)-cholestenoic acid (crystallized ligand) as shown in Figure 2.

In addition, in silico screening of all compounds from NL showed that benene-1,2,4-Trimethyl exhibited the lowest binding energy of -10.7 among all the compounds examined as shown in Figure 3.

Table 4: *In vitro* Antioxidant Properties of *Euphorbia hirta* and *Nauclea latifolia* leaves

Parameters	*Euphorbia hirta*	*Nauclea latifolia*
DPPH (EC_{50})(µg/mL)	1.13	1.63
FRAP (mMFe^{++}/Kg)	0.22	0.34
ORAC (% Inhibition)	55.26	61.63

Keys:
DPPH: 2,2-Diphenyl-1-Picrylhydrazyl
FRAP: Ferric Reducing Antioxidant Power
ORAC: Oxygen Radical Absorbance Capacity

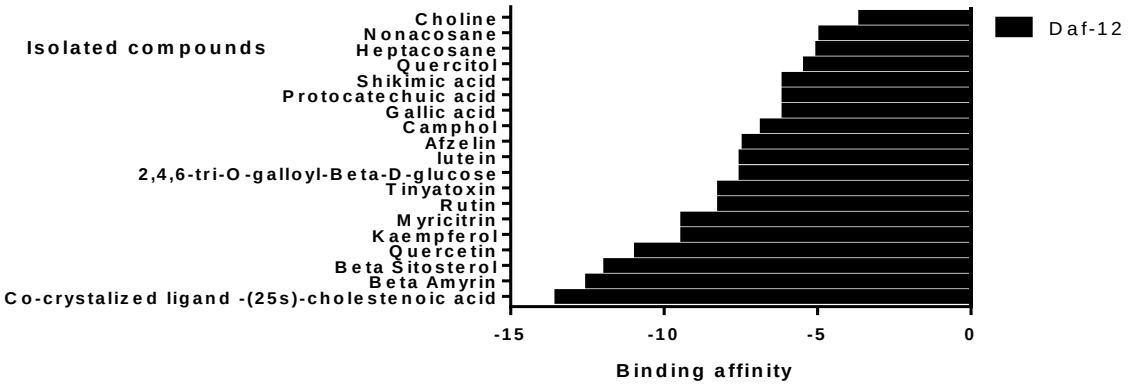

Figure 2: Binding affinity of compounds isolated from *E. hirta* with Daf-12 receptor

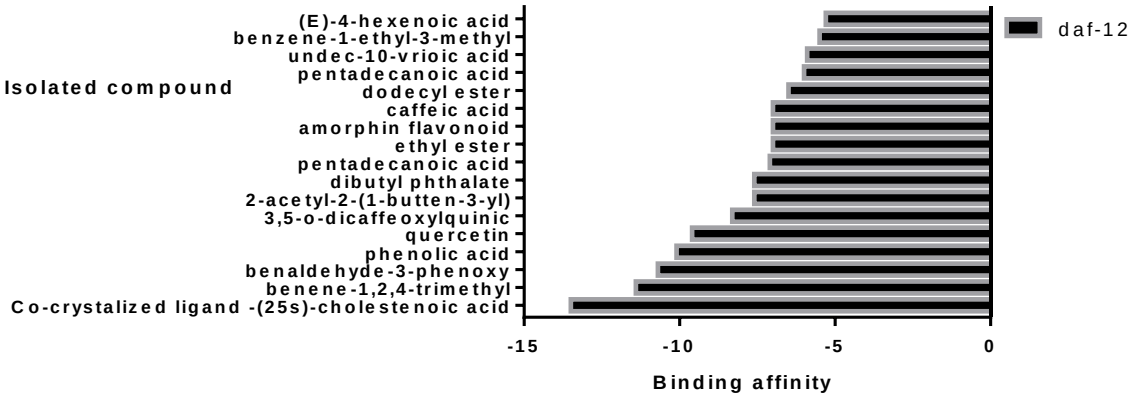

Figure 3: Binding affinity of compounds isolated from *N. latifolia* with Daf-12 receptor

Table 5: Anthelmintic activities of methanol leaf extracts of *Euphorbia hirta* and *Nauclea latifolia* leaves

Extracts	Concentration	*Taenia solium*		*Pheritima pasthuma*		*Fasciola gigantica*	
		P	D	P	D	P	D
E. hirta	10	35 ± 0.1	62 ± 0.3	16 ± 0.7	60 ± 0.2	23 ± 0.8	61 ± 0.1
	30	27 ± 0.7	59 ± 0.4	12 ± 0.1	56 ± 0.7	18 ± 0.2	58 ± 0.7
	50	18 ± 0.2	43 ± 0.7	7 ± 0.2	41 ± 0.3	10 ± 0.7	42 ± 0.2
N. latifolia	10	30 ± 0.2	61 ± 0.2	16 ± 0.5	55 ± 0.2	21 ± 0.1	58 ± 0.2
	30	21 ± 0.6	58 ± 0.3	10 ± 0.8	48 ± 0.1	15 ± 0.7	42 ± 0.1
	50	8 ± 0.1	42 ± 0.4	6 ± 0.1	30 ± 0.2	9 ± 0.8	25 ± 0.7
Antepar	10	8 ± 0.1	41 ± 0.4	18 ± 0.2	52 ± 0.1	3 ± 0.2	5 ± 0.1
Distilled water	50	-	2280	-	2520	-	300

Table 6: Anthelmintic activities of Hexane leaf extracts of *Euphorbia hirta* and *Nauclea latifolia* leaves

Extracts	Concentration	*Taenia solium*		*Pheritima pasthuma*		*Fasciola gigantica*	
		P	D	P	D	P	D
E. hirta	10	36 ± 0.4	64 ± 0.1	19 ± 0.3	62 ± 0.1	28 ± 0.5	65 ± 0.2
	30	30 ± 0.2	62 ± 0.5	14 ± 0.7	59 ± 0.6	20 ± 0.2	60 ± 0.7
	50	15 ± 0.6	45 ± 0.1	10 ± 0.4	43 ± 0.2	11 ± 0.3	48 ± 0.1
N. latifolia	10	31 ± 0.1	65 ± 0.7	18 ± 0.3	56 ± 0.1	25 ± 0.1	58 ± 0.2
	30	19 ± 0.2	60 ± 0.2	13 ± 0.5	50 ± 0.4	18 ± 0.3	48 ± 0.2
	50	13 ± 0.1	40 ± 0.5	8 ± 0.3	32 ± 0.2	12 ± 0.1	30 ± 0.7
Antepar	10	8 ± 0.1	41 ± 0.4	18 ± 0.2	52 ± 0.1	3 ± 0.2	5 ± 0.1
Distilled water	50	-	2280	-	2520	-	300

Molecular interaction of Beta-amyrin, Benzene-1,2,4-trimethyl and co-crystallized ligand

Molecular interactions of Beta amyrin with daf-12 nuclear receptor

Figures 4A and 4B showed the interaction between beta-Amyrin and the daf-12 protein in 3D and 2D format respectively. From the 2D interaction it was observed that there are three different interactions involved in the binding of the drugmolecule with the protein (daf-12) which are van der Waal interaction, conventional Hydrogen bonding and pi sigma interaction.

Results of swissADME of most effective compound

Results obtained from docking of compounds isolated from EH and NL, showed that beta-amyrin is the hit compound against daf-12 nuclear receptor. Physicochemical characterization of beta-amyrin showed that the compound possesses a molecular weight of 426.72 g/mol, a heavy atom of 31, no rotatable bond and aromatic heavy atoms as shown in Table 7.

The aqueous solubility of beta-amyrin showed that the compound is poorly soluble in an aqueous medium, hence the suspected promising effect against the lipid/membrane-rich daf-12 nuclear receptor details are shown in Table 8.

Findings from Table 9 showed that beta-amyrin possesses a lipophilic property, which might have contributed to the ability of the compound to bind to the target receptor which is a nuclear receptor that is associated with lipids.

Low gastrointestinal absorption and inability to cross blood - brain barrier were observed with the hit compound (beta-amyrin). In addition, the compound was also observed to have no inhibitory influence on some key drug metabolising enzymes such as CYP1A2 etc as shown in Table 10.

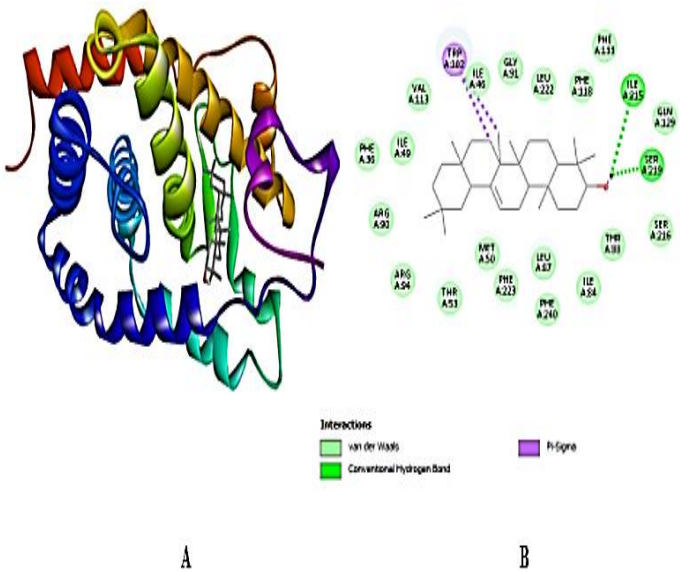

Figure 4A - B: Molecular interaction of β Amyrin with nuclear receptor Daf-12
A – 3D interaction of beta-Amyrin with Daf-12
B – 2D interaction of beta-Amyrin with Daf-12

Table 7: Physicochemical properties of beta-amyrin isolated (hit compound) from *E. hirta*

S/N	Compound Name	Molecular Weight g/mol	Heavy Atoms	TPSA	Rotatable Bonds	H-Bond Acceptor(s)	H-Bond Donor(s)	Molecular Refractivity	Fraction CSp^3	Aromatic Heavy atom
1	β-Amyrin	426.72	31	20.23	0	1	1	134.88	0.93	0

Table 8: Aqueous solubility of beta-amyrin isolated (hit compound) from *E. hirta*

S/N	Compound Name	Log S (ESOL)	Class	Log S (Ali)
1	β-Amyrin	-8.25	Poorly soluble	-9.47

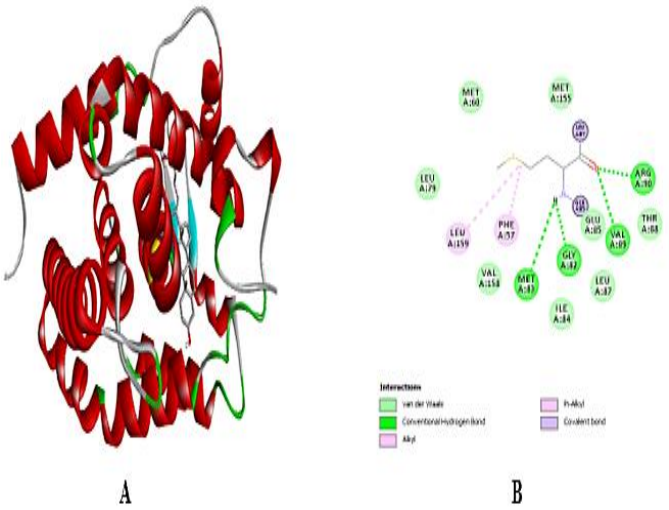

Figure 5A - B: Molecular interaction of (25s)-cholestenoic (co-crystalized ligand) with nuclear receptor Daf-12
A - 3D interaction of (25s)-cholestenoic (co-crystalized ligand) with daf-12; B - 2D interaction of (25s)-cholestenoic (co-crystalized ligand) with daf-12

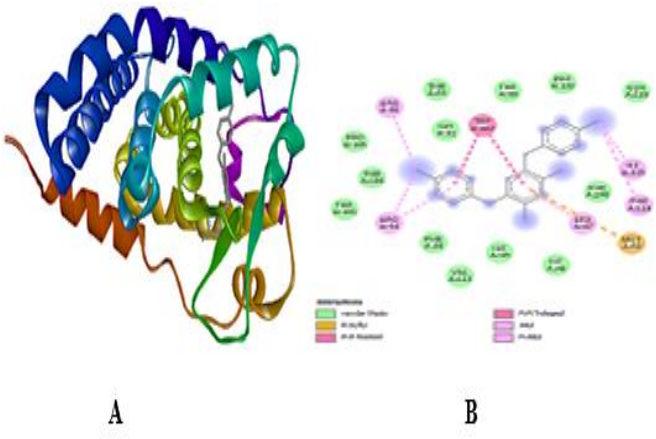

Figure 6A - B: Molecular interaction of Benene-1, 2,4-Trimethylwith nuclear receptor Daf-12
A - 3D interaction of benene-1,2,4-trimethylwith daf-12; B - 2D interaction of benene-1,2,4-trimethyl with daf-12

Molecular Dynamics (MD) Simulations
Root Mean Square Deviation (RMSD)
Root Mean Square Deviation (RMSD) helps in the determination of the union and stability of the two complexes and the unbound protein.45 Long MD simulations time is essential for a complex system to attain stability. An increase in the values of RMSD indicates that there is more atomistic deviation, while a low RMSD value indicates complex with a minimal structural abnormality and highly stable46; as shown from Figure 7 the estimated average RMSD values were 1.57 Å, 1.70 Å, and 1.72 Å for control-bound, beta amyrin-bound and the unbound protein complexes respectively. The results displayed that all the systems exhibited an average RMSD up to ~1.7Å at maximum, signifying a comparatively stable simulation. Similarly, the systems attained convergence virtually throughout the entire 200 ns simulation period. The results of the RMSD revealed that the binding of the control had a more stabilizing effect than Ligand and unbound-conformation. The highly stable binding pocket residues detected in the control bound could have favoured a steadier residue interaction with control and probably stronger binding to the protein relative to ligand.[47]

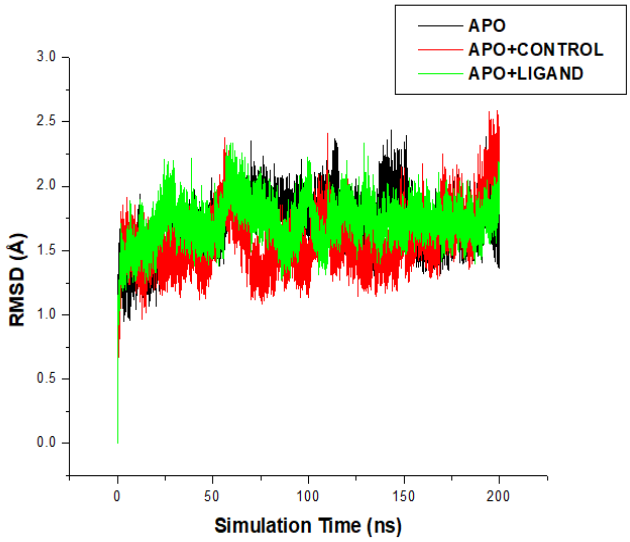

Figure 7: The RMSD for the complexes

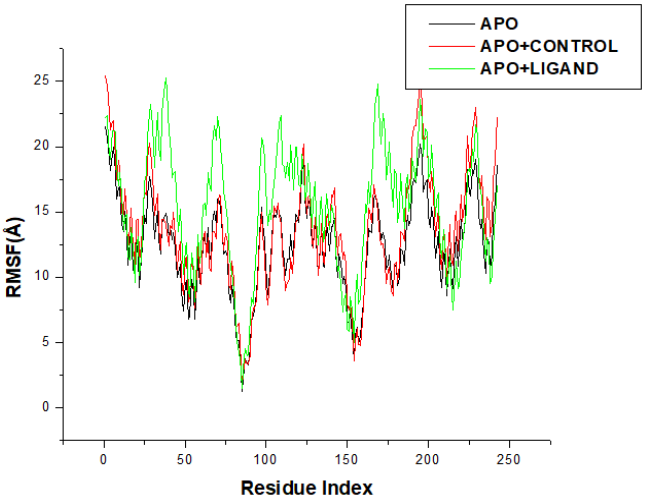

Figure 8: The RMSF of the complexes

Root Mean Square Fluctuation (RMSF)

Root Mean Square Fluctuation (RMSF) analysis gives understanding of the elasticity of the complex structure by evaluating the fluctuation of each amino acid existing in the protein. The conformational dynamics of the residues of the protein perform a significant role in the function of the protein.48 The analysis of RMSF offers a better understanding of the fluctuations in conformation upon ligand binding and illustrates the implication of molecular dynamics at the atomistic level. The MD simulations trajectories in attaining the RMSF disclosed the alterations in the residues' flexibilities with or without a ligand. The RMSF was calculated for the residues that were established in the protein upon binding of the control and ligand to observe their effect on the conformational dynamics. The elevated values of RMSF showed more flexible activities, whereas the lower fluctuation values demonstrated lesser conformational changes upon the simulation.[45] The average RMSF values of control-bound, ligand-bound and the unbound protein complexes were 13.5Å, 15.5 Å and 12.4 Å respectively (Figure 8). As shown, unbound protein had the least residue variability compared to control and ligand, suggesting increased protein residue variability upon control and ligand binding. Furthermore, the lower RMSF value for unbound protein compared to both control and ligand complexes may be indicated in the system's compactness.

Radius of Gyration (RoG)

RoG helps to estimate the compactness of the entire protein structure during the course of the simulation.48 The rigidity or slackness of the protein structure has the ability to interfere with its biological properties. It has been reported that the relationship between C- α RoG and compactness of protein structure revealed that forfeiture in structural compactness is as a result of high RoG value, and structurally compact protein is as a result of a low RoG value.49 We also predicted the effects of binding of control and ligand on the compactness of the protein active site across the period of MD simulations. The average RoG values of control-bound, Ligand-bound and the unbound protein complexes were 18.3 Å, 18.2 Å, and 18.1 Å respectively (Figure 9), showing very similar compactness for the three systems. On the other hand, the results showed the atomic allocations in the unbound protein to indicate low RoG value and low compactness, which is correlative with the low RMSF value obtained. The high RoG observed in the conjugated system indicates that control and ligand binding resulted in a slightly looser protein conformation compared to the unconjugated system.

Snapshot

The Snapshot of interactions at different simulation times of both the control and the ligands with the protein are shown below. It was observed that there are differences in the residue's interaction in both the control and ligand which may account for their stability and compactness.

Plant antioxidants, in recent years have become an object of renewed interest, probably because of side effects of some commercial antioxidants which is undesirable. Medicinal plants have been endowed with diverse quantities of various kinds of bioactive chemical compounds having antioxidant properties which play a major role in stopping free radical chain reactions from being generated. Diphenyl Picryl Hydrazine (DPPH), a stable synthetic free radical has been used widely for determining natural compounds' antioxidant activities.11,40,41 The DPPH is an ideal method due to it being easy, consistent and fast; water, methanol or ethanol do not also disintegrate it. Hence, in this study, E. hirta and N. latifolia as potential antioxidant agents were tested for their radical scavenging and antioxidant activities by DPPH.11,16 The DPPH scavenging assay finds its basis on the methanol DPPH solution's reduction when Hydrogen donating antioxidant is present leading to a non-radical form DPPH-H (Diphenyl Picryl Hydrazine) been formed. A change in colour from purple to yellow occurs which is proportional to the concentration and scavenging potential of the extract in terms of Hydrogen donating ability.[11] The EC50 was the value calculated been the amount of antioxidant present in the sample needed to decrease the initial DPPH concentration by 50%. Antioxidant activity is higher when the EC50 value is lower. Euphorbia hirta leaf extract had the lowest EC50 value due to their high antioxidant activities. In the present study, N. latifolia leaf extracts exhibited higher percentage inhibition than Euphorbia hirta leaf extracts. Three comparable, complementary antioxidant assays were used in studying the quantitative antioxidant activities of E. hirta and N. latifolia leaf samples which were DPPH Free Radical Scavenging ability, Ferric Reducing Antioxidant Power (FRAP) and Oxygen Radical Absorbance Capacity (ORAC). Nauclea latifolia leaf samples exhibited a higher DPPH value (1.63 µg/mL) compared to E. hirta (1.13 µg/mL) (Table 4). This corroborates the quantitative antioxidant assay in the study carried out by.8, 42 Results indicated that N. latifolia leaf sample was a better antioxidant agent compared to E. hirta leaves in its capacity to scavenge free radicals in the DPPH assay. The Ferric Reducing Antioxidant Power (FRAP) of N. latifolia and E. hirta were 3.43 mMFe++/Kg and 2.22 mMFe++/Kg respectively, still confirming N. latifolia as a better antioxidant agent. Oxygen Radical Absorbance antioxidant activities Capacity (ORAC) values of N. latifolia and E. hirta leaves were 61.6 % and 55.26 % respectively further proving N. latifolia leaves as a better antioxidant agent having a higher antioxidant activity (Table 4). Oxygen Radical Absorbance Capacity (ORAC) and FRAP values of E. hirta and N. latifolia leaves were significantly different at $p<0.05$ while DPPH values for the two plant leaf samples showed no significant difference at $p<0.05$.

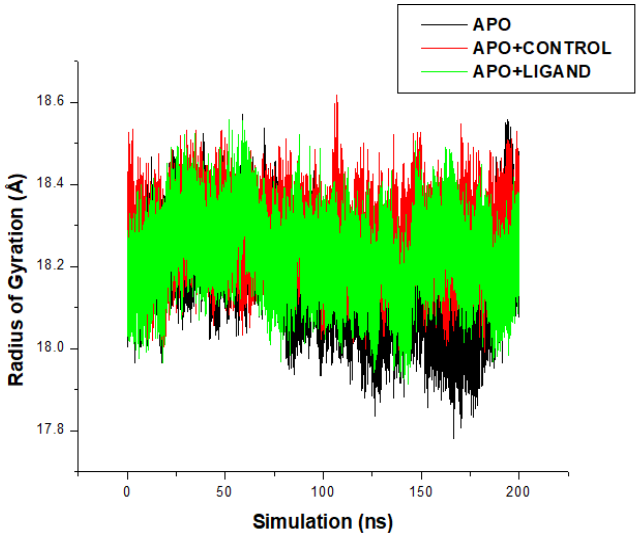

Figure 9: The RoG of the complexes

Table 9: Lipophilicity of beta-amyrin isolated (hit compound) from *E. hirta*

S/N	Compound Name	iLog P	XLog P_3	WLog P (Log Po/w)	MLog P	Silicos-ITLog P	Concensus (Log Po/w)
1	β-Amyrin	4.74	9.15	8.17	6.92	6.92	7.18

Table 10: Pharmacokinetic Study of Compound Isolated from *E. hirta*

S/N	Compound Name	GI absorption	BBB Permeant	P-gp substrate	CYP1A2 inhibitor	CYP2C19 inhibitor	CYP2C9 inhibitor	CYP2D6 inhibitor	CYP3A4 inhibitor	Log Kp (cm/s)
1	β-Amyrin	Low	No	No	No	No	No	No	No	-2.41

The mineral analyses of E. hirta and N. latifolia leaves as presented in Table 3 showed the presence of micro and macro nutrients in reasonable quantities in the two plants. In this study, it was observed that E. hirta was a richer source of most essential minerals as shown in Table 3 with Calcium value being 140.60 ppm compared to 92.25 ppm in N. latifolia; Potassium in E.hirta was 2896.00 ppm as compared to 314.80 ppm in N. latifolia; Sodium in E.hirta was 161.55 ppm compared to 108.35 ppm in N. latifolia; Zinc in E.hirta amounted to 9.42 ppm while 6.128 ppm was found in N. latifolia; Iron in E.hirta amounted to 13.02 ppm while 0.396 ppm was found in N. latifolia; Copper in E. hirta had a value of 0.530 ppm as compared to 0.742 ppm in N. latifolia; Manganese in E.hirta amounted to 2.69 ppm while 0.446 ppm of Manganese was found in N. latifolia; Chromium in E. hirta amounted to 0.10 ppm while 0.031 ppm was found in N. latifolia. Sodium and Potassium as the major extra cellular and intracellular minerals are involved in body water balance and acid-base balance. Hyponatremia is the result of failure to consume sufficient Sodium when fluid and Sodium losses are high. They are also involved in the transport of some non-electrolytes.22 Serious disorders like headache, tiredness, muscle cramps in the body can result from the maintenance of osmotic equilibrium by Sodium (Na).[22] Calcium is majorly found in the skeleton; the two plant leaves are rich in Calcium as it was present at high values in them. Bone forming and maintenance, muscle contraction and blood clotting are done by Calcium. A large number of enzymes are formed by Zinc, many of which function in wound healing and energy metabolism.22 DNA synthesis, storage, release, function of insulin and the development of sexual organs and bones are also achieved by Zinc. Iron is necessary for the formation of haemoglobin. Poor Oxygen-carrying capacity, a condition causing endurance problems in athletes, is a characteristic of Iron deficiency or Anaemia. Bone and teeth formation need Phosphorus as an essential element. Manganese, a trace mineral is involved in bone formation, antioxidant activity, immune function and carbohydrate metabolism. Paralysis and convulsion may result as its deficiency. Potassium and Calcium were the most abundant mineral nutrients in the leaves of both plants used for this study. However, the elemental concentrations in both plants may be a reflection of the elemental composition of their parent soils.15 The statistical results of the mineral analyses showed that Sodium, Calcium, Potassium, Magnesium, Iron, Manganese, Zinc, Copper and Chromium of E. hirta and N. latifolia leaves were significantly different at $p<0.05$ while Lead and Selenium showed no significant difference at $p<0.05$.

Most worm expellers like antepar functions to paralyze worms so that they are expelled in the faeces of both man and animals. The extracts, apart from causing paralysis to worms used, also caused their death, mostly at 50 mg/mL being the highest concentration used. As shown in Tables 5 and 6, the three concentrations of methanol and hexane leaf extracts of E. hirta and N. latifolia used (10, 30 and 50 mg/mL) exhibited profound anthelmintic activities. The anthelmintic activities of the plant extracts were dependent on concentrations for the three worm types (Pheritima pasthuma, Taenia solium and Fasciola gigantica) used for this study; with the shortest time of paralysis (P) and death (D) achieved at 50 mg/mL for the three worm types used. This result corroborates some scientific findings.[24, 25, 27]

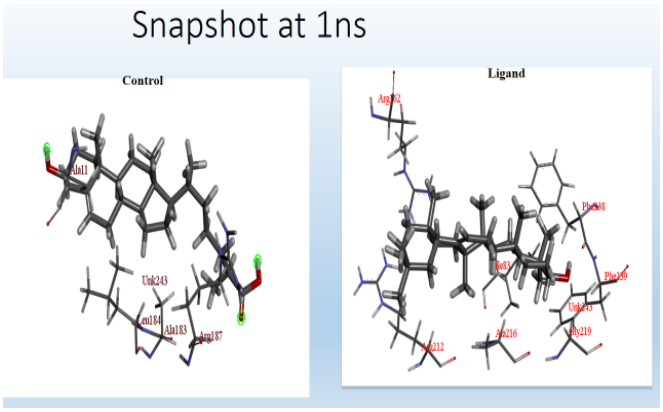

Figure 10A: The snapshot of the control and the ligands at 1ns

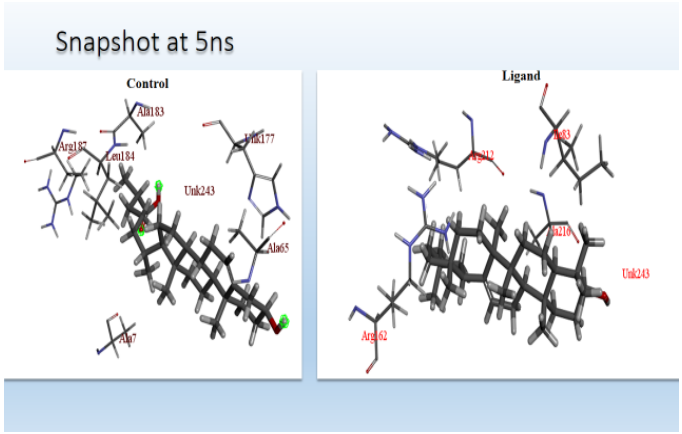

Figure 10B: The snapshot of the control and the ligands at 5ns

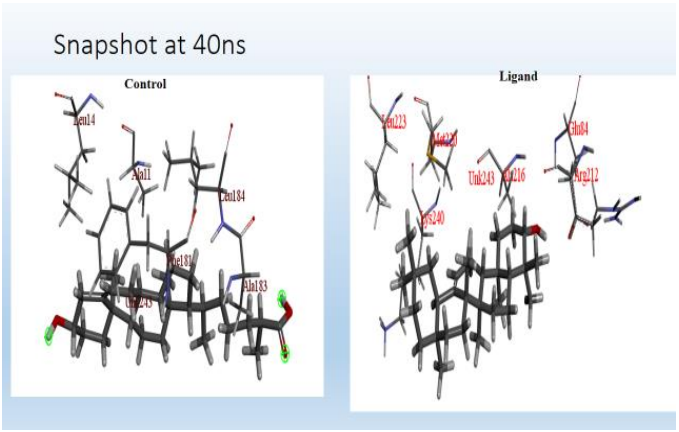

Figure 10C: The snapshot of the control and the ligands at 40ns

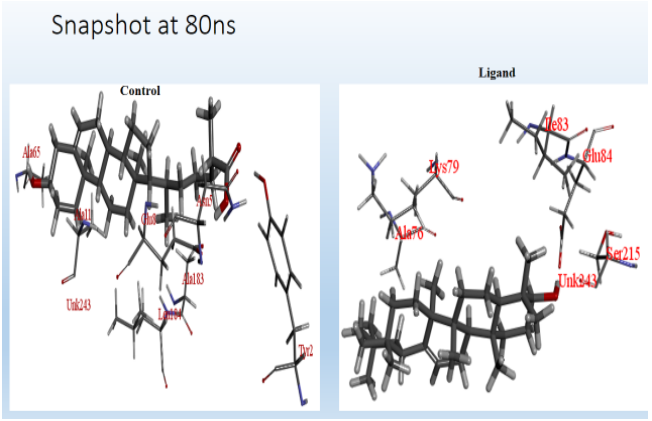

Figure 10D: The snapshot of the control and the ligands at 80ns

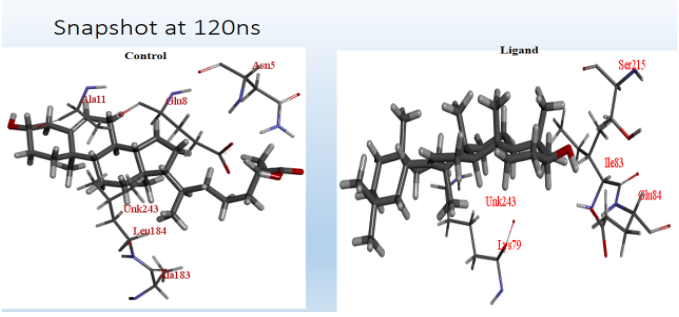

Figure 10E: The snapshot of the control and the ligands at 120ns

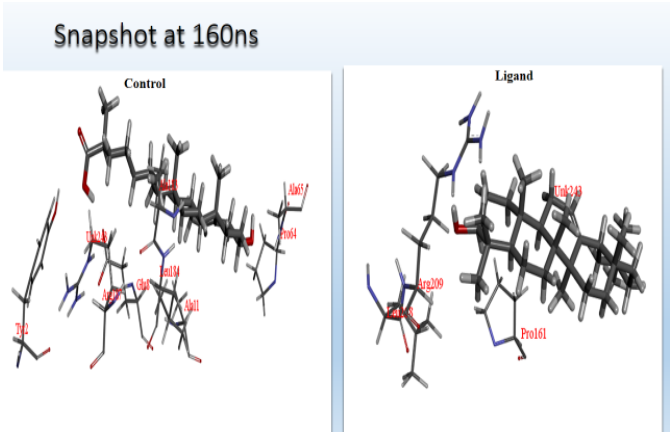

Figure 10F: The snapshot of the control and the ligands at 160ns

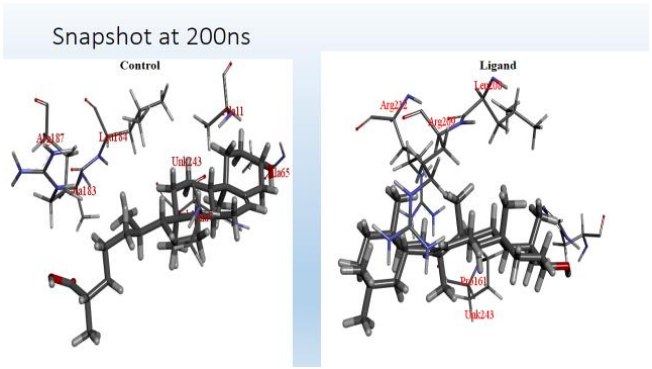

Figure 10G: The snapshot of the control and the ligands at 200ns

Tables 5 and 6 showed that methanol leaf extract of N. latifolia had a higher anthelmintic activity than the methanol leaf extract of E. hirta for the three worm types used; while hexane leaf extract of N. latifolia showed a higher anthelmintic activity than the hexane leaf extract of E. hirta for the three types of worms used. Generally, methanol leaf extract of N. latifolia exhibited the highest activity than other extracts used in the study. Pheritima pasthuma was most susceptible (sensitive) to the methanol leaf extract of N. latifolia (Table 5). It was paralysed within 6 minutes and died 30 minutes after the administration of N. latifolia methanol leaf extract; while paralysis (P) and death (D) times of P. pasthuma with the standard drug (Antepar) were 18 and 52 minutes respectively. Pheritima pasthuma was not easily killed by E. hirta hexane leaf extract (Table 6).

Euphorbia hirta methanol leaf extracts exhibited appreciable anthelmintic properties with T. solium. Taenia solium were paralyzed or died within 15-43 minutes of plant extracts administration while the worms were paralyzed or died within 5-43 minutes of the administration of 10 mg/mL dose of Antepar, a standard anthelmintic drug used as control. Another control group (worms in distilled water), lived for about 48 hours (Tables 5 and 6). Hexane leaf extract of N. latifolia showed highest anthelmintic activity against P. pasthuma with time of paralysis (P) = 8 mins and time of death (D) = 32mins while paralysis and death times for the standard or reference drug (Antepar) were 18 and 52 mins respectively (Table 6). Pheritima pasthuma was most sensitive to N. latifolia leaf extracts concentrations of 10, 30 and 50 mg/ml with time of paralysis (P) = 18±0.3, 13±0.5 and 8±0.3 minutes and death (D) = 56±0.1, 50±0.4 and 32±0.2 minutes respectively for hexane leaf extracts of N. latifolia; and with time of paralysis (P) = 16±0.5, 10±0.8 and 6±0.1 minutes and death (D) = 55±0.1, 48±0.1 and 30±0.2 minutes respectively for methanol leaf extracts of N. latifolia (Table 6). Generally, P. pasthuma was the most susceptible to the two plant leaf extracts, especially when compared to the standard drug, Antepar (10 mg/mL) at 50 mg/mL, paralysis time (P) for the earthworms was between 8–10 mins and death time (D) also in between 32–60 minutes. The extracts were more effective in causing paralysis of T. solium (tapeworms) at 50 mg/ml rather than death. This result is also in line with the results.[27]

Times of paralysis and death were 18-45 mins for E. hirta hexane leaf extract; and 13-40 mins for N. latifolia hexane leaf extract; while for the reference drug, paralysis time (P) and death (D) was 8-41 mins (Table 6). The methanol extracts of N. latifolia showed reasonable anthelmintic properties with F. gigantica which became paralysed and eventually died between 10–42mins; while F. gigantica in E. hirta methanol leaf extract was paralysed and died between 9-25mins at a concentration of 50mg/mL. Antepar also paralysed and killed the worms between 3-5 mins. Control (worms in distilled water) survived for a period of 48h (Table 5). Both E. hirta and N. latifolia hexane leaf extracts at 50 mg/mL concentration was also worthy of note; as Fasciola gigantica was paralysed and died between 11-48 mins with E. hirta hexane leaf extract while they were paralysed and died between 12-30 mins with N. latifolia hexane leaf extract. Antepar paralysed and killed the worms around 3-5 mins. Fasciola gigantica in distilled water (control) lived for a period of 42h (Table 6).

However, molecular docking of compounds reportedly isolated from E. hirta and N. latifolia against daf-12 nuclear receptor showed that beta-Amyrin from E. hirta had a promising effect with the lowest binding affinity of -11.90 (Figure 3). The compound also had Hydrogen bond, van der Waals and pi- sigma interactions with some Amino acid residues in the binding site of the receptor (Figure 4A – B). Also, Benzene-1,2,4-trimethyl from N. latifolia showed a promising result (-10.7), which is higher than binding affinity of beta amyrin (-11.70), hence the lower activity of benzene-1,2,4-trimethyl relative to beta amyrin (Figures 2, 5A and 5B).

Apart from antioxidant, anti-inflammatory, antinociceptive, literature search showed no information relating beta-Amyrin to anthelmintics or daf-12 nuclear receptor, based on this promising role of beta-Amyrin, the compound can be a good drug candidate but might have challenges of gastrointestinal absorption as shown in Tables 7.[10. 33,43]

The structures and dynamics of biomolecules are vital facts provided by the approach of MD simulations and also help in the design of a potent drug. The arrangement of a protein structure is an important factor for its physiological activity; consequently, the arrangements could lead to positive or negative outcome on the activities of such protein when their structural integrity undergoes alteration.49 As a result of this effect, co-crystalized-bound, beta amyrin-bound and the unbound protein complexes undergoes MD simulations of about 200 ns to investigate the energetics of each complex and confirm the convergence of dynamic stability. Trajectories obtained from the simulated systems were further examined for RMSD and RMSF to understand the structural dynamics and equilibrium during interaction and binding. The RoG and snapshot were also analysed for further understanding of the complexes as shown in Figures 7 – 10. The RMSD results provide information that the binding of the control process more stable effect on the binding domain than ligand (beta amyrin) and protein alone (unbound-conformation).[50,51] The favourable stability of binding pocket of Amino acids was obtained in the (25s)-cholestenoic (control/native ligand) bound could be ideal for tightly bounded residue interaction with control and perhaps stronger binding to the protein relative to ligand (Figure 7). RMSF (Root Mean Square Variation) results demonstrate data demonstrating lower amino acid variation for unbound protein compared to (25s)-cholestate (control/native ligand) and ligand (β-amyrin), indicating that the protein undergoes an increase in conformation in the course of binding controls and ligands (Figure 8). Furthermore, the lower RMSF values of the unbound protein compared to controls and ligand complexes could be due to the system's compactness.52 However, the RoG result revealed that the atomic distributions in the unbound protein have a low RoG value (Figure 9) and low compactness, which correlated with the low RMSF value obtained in Figure 8. The high RoG was observed in the bound (beta amyrin and native ligand)-complexes indicated that the binding of control and ligand led to a little looser protein conformation relative to the unbound protein.[53,54]

Conclusion

Conclusion therefore can be drawn that *E. hirta* and *N. latifolia* exhibited reasonable anthelmintic properties which back up their uses in ethnobotany (phytomedicine) as anthelmintic recipes. The dauer diapause effect on all the worms examined in the research might be due to antagonistic effect induced by multiple interactions between beta-Amyrin from *E. hirta* and Benzene-1,2,4-trimethyl from *N. latifolia* and some key Amino acids in the binding site of daf-12 nuclear receptor..

Conflict of Interest

The authors declare no conflict of interest.

Authors' Declaration

The authors hereby declare that the work presented in this article is original and that any liability for claims relating to the content of this article will be borne by them.

Acknowledgments

Authors hereby acknowledge the help of Mr. D. Olalekan of the Zoology and Environmental Science Department of Ekiti State University, Ado-Ekiti, Nigeria for his assistance in identifying the worms used and rendering assistance in carrying out the anthelmintic studies

References

1. Charlier J, Bartley DJ, Sotiraki S, Martinez-Valladares M, Claerebout E, von Samson-Himmelstjerna G, Thamsborg SM, Hoste H, Morgan ER, Rinaldi L. Anthelmintic resistance in ruminants: challenges and solutions. Adv Parasitol. 2022 ;115:171-227. doi: 10.1016/bs.apar.2021.12.002
2. Wolstenholme AJ. Ion channels and receptor as targets for the control of parasitic nematodes. Vol. 1, International Journal for Parasitology: Drugs and Drug Resistance. 2011. p. 2–13.
3. Wang Z, Schaffer NE, Kliewer SA, Mangelsdorf DJ. Nuclear receptors: Emerging drug targets for parasitic diseases. J. Clin Invest. 2017; 127(4):1165–71.
4. Williamson SM, Robertson AP, Brown L, Williams T, Woods DJ, Martin RJ, et al. The nicotinic acetylcholine receptors of the parasitic nematode Ascaris suum: Formation of two distinct drug targets by varying the relative expression levels of two subunits. PLoS Pathog. 2009;5(7):e1000517.
5. Frayha GJ, Smyth JD, Gobert JG, Savel J. The mechanisms of action of antiprotozoal and anthelmintic drugs in man. Gen Pharmacol. 1997; 28(2):273–99.
6. Rose VH, Morgan ER, Hertzberg H, Bartley DJ, Bosco A, Charlier J, Chartier C, Claerebout E, de Waal T, Hendrickx G, Hinney B, Höglund J, Ježek J, Kašný M, Keane OM, Martínez-Valladares M, Mateus TL, McIntyre J, Mickiewicz M, Munoz AM, Phythian CJ, Ploeger HW, Rataj AV, Skuce PJ, Simin S, Sotiraki S, Spinu M, Stuen S, Thamsborg SM, Vadlejch J, Varady M, von Samson-Himmelstjerna G, Rinaldi L. Increasing importance of anthelmintic resistance in European livestock: creation and meta-analysis of an open database. Parasite. 2020; 27:69. doi: 10.1051/parasite/2020062
7. Ghosh P, Ghosh C, Das S, Das C, Mandal S, Chatterjee S. Botanical Description, Phytochemical Constituents and Pharmacological Properties of Euphorbia hirta Linn: A Review. Int J Heal Sci Res. 2019;9.
8. Abiodun F, Igwe A, Osahon O. Anti-microbial evaluation of a herbal dental remedy: Stem bark of Nuclea latifolia-family rubiaceae. J. Appl Sci. 2007;7(18): 2696-2700.
9. Oshadie G, Silva D, Abeysundara AT, Minoli M, Aponso W. Extraction methods, qualitative and quantitative techniques for screening of phytochemicals from plants. ~ 29 ~ Am J Essent Oils Nat Prod. 2017;5(2): 29-32.
10. Gospel Ajuru M. Qualitative and Quantitative Phytochemical Screening of Some Plants Used in Ethnomedicine in the Niger Delta Region of Nigeria. J Food Nutr Sci. 2017;5(5): 198.
11. Oluwasegun A. In Vitro Free Radical Scavenging Activity and Total Phenolic Content of Kigelia Africana (LAM). Int J Sci Res. 2014;3(1): 368-70.
12. Cardoso-Gutierrez E, Aranda-Aguirre E, Robles-Jimenez LE, Castelán-Ortega OA, Chay-Canul AJ, Foggi G, Angeles-Hernandez JC, Vargas-Bello-Pérez E, González-Ronquillo M. Effect of tannins from tropical plants on methane production from ruminants: A systematic review. Vet Anim Sci. 2021; 9;14:100214. doi: 10.1016/j.vas.2021.100214
13. Christiana Jesumirhewe, Adaobi Sandra Okoro, Oluwasegun Adedokun. The phytochemical constituents and antibacterial activity of methanolic and ethanolic leaf and stem extracts of Eucalyptus torelliana, Nigeria. GSC Biol Pharm Sci. 2021; 16(2): 306-311. https://doi.org/10.30574/gscbps.2021.16.2.0246
14. Nasiru A, Oluwasegun A. Phytochemical, nutritional and amino acid composition of Citrullus lanatus (Cucurbitaceae) seeds cultivated in South-South Nigeria. ~ 3738 ~ J Pharmacogn Phytochem. 2019;8(3):3738–40.
15. Adedokun O, Gbolade A, Ayinde B. 13, 14-Epoxyoleanan-3-ol-acetate: A male fertility enhancing constituent from hexane fraction of Momordica charantia Linn (Curcubitaceae). Turkish J Pharm Sci. 2021; 0(0): 180-186. doi: 10.4274/tjps.galenos.2021.48264
16. Ayofe AM, Oluwasegun A, Adesina AB, Ogochukwu U. Comparative studies on In-vitro radical scavenging potential of methanol extracts of Garcinia kola heck (Clusiaceae) seeds, Conyza sumatrensis retz (Asteraceae) and Mitracarpus scaber zucc (Rubiaceae) leaves. ~ 33 ~ Am J Essent Oils Nat Prod. 2017; 5(2):33–6.
17. Samatha T, Srinivas P, Shyamsundarachary R, Rajinikanth M, Rama Swamy N. Phytochemical analysis of seeds, stem bark and root of an endangered medicinal forest tree OROXYLUM INDICUM(L)kurz. Int J Pharma Bio Sci. 2012; 3(3):B1063-B1075.
18. Mansor N, Herng HJ, Samsudin SJ, Sufian S, Uemura Y. Quantification and Characterization of Allicin in Garlic Extract. J Med Bioeng. 2016; 5(1):24–7.
19. Khanal S. Qualitative and Quantitative Phytochemical Screening of Azadirachta indica Juss. Plant Parts. Int J Appl Sci Biotechnol. 2021;9(2): 122-127. DOI: 10.3126/ijasbt.v9i2.38050
20. Harris R. Anglo-Saxon aromatherapy: its evolution and current situation. Int J Aromather. 2003;13(1): 9-17.
21. Evans WC. Trease and Evans Pharmacognosy. 15th edtion. Edinburgh, Saunders. 2002.
22. Ogunmefun OT, Fasola TR, Saba AB, Oridupa OA. The ethnobotanical, phytochemical and mineral analyses of Phragmanthera Incana (Klotzsch), a species of mistletoe growing on three plant hosts in South-western Nigeria. Int J Biomed Sci. 2013; 9(1):33-40.
23. Oluwasegun A, Ume O, Nasiru A, Peter A, Benjamin G. Evaluation of antidiabetic and anti-lipid peroxidation potentials of leaves crude and solvent fractions of Annona muricata Linn (Annonaceae). 2019; 8(3):3973–7.
24. Boly1 AG., Belemlilga M., Traore A, S Ouedraogo E, Guissou I. Phytochemical Study and In vitro Anthelminthic Properties Studies of the Trunk Barks Aqueous Extract from Acacia Nilotica Var. Adansonii (Guill & Perr). O Ktze (Mimosaceae). Int J Pharmacogn Phytochem Res. 2018;10(1):5-10.
25. Oliveira Santos F, Ponce Morais Cerqueira A, Branco A, José Moreira Batatinha M, Borges Botura M. Anthelmintic activity of plants against gastrointestinal nematodes of goats: A review. Vol. 146, Parasitology. 2019. 158pp.

26. Ngouateu Teufack SE, NMbogning Tayo G, Ngangout Alidou M, Yondo J, Djiomene AF, Wabo Poné J, Faùily Mpoame Mbida. Anthelminthic properties of Methylene chloride-methanol (1:1) extracts of two Cameroonians medicinal plants on Heligmosomoides bakeri (Nematoda: Heligmosomatidea). BMC Complement Altern Med. 2017;17(1):630-634. https://doi.org/10.1186/s12906-017-1908-8
27. Ajayeoba OO, Diehl DL. Pneumatic dilation for achalasia: new techniques to improve an old procedure. VideoGIE. 2020;5(10).
28. Bintari YR, Risandiansyah R. In Silico Study to Assess Antibacterial Activity from Cladophora Sp. on Peptide Deformylase: Molecular Docking Approach. Borneo J Pharm. 2019;2(1):20-23.
29. Simon L, Imane A, Srinivasan KK, Pathak L, Daoud I. In Silico Drug-Designing Studies on Flavanoids as Anticolon Cancer Agents: Pharmacophore Mapping, Molecular Docking, and Monte Carlo Method-Based QSAR Modeling. Interdiscip Sci Comput Life Sci. 2017 Sep 1;9(3):445–58.
30. Oso BJ, Adeoye AO, Olaoye IF. Pharmacoinformatics and hypothetical studies on allicin, curcumin, and gingerol as potential candidates against COVID-19-associated proteases. J Biomol Struct Dyn. 2022;40(1):1 -7.
31. Muh'd M baba, Uzairu A, Shallangwa GA, Uba S. Molecular docking and quantitative structure-activity relationship study of anti-ulcer activity of quinazolinone derivatives. J King Saud Univ - Sci [Internet]. 2020;32(1).657–666 Available from:https://doi.org/10.1016/j.jksus.2018.10.003
32. Saeed M, Shoaib A, Tasleem M, Alabdallah NM, Alam MJ, El Asmar Z, et al. Assessment of antidiabetic activity of the shikonin by allosteric inhibition of protein-tyrosine phosphatase 1b (Ptp1b) using state of art: An in silico and in vitro tactics. Molecules. 2021;26(13). 10.3390/molecules26133996
33. Abdul-Hammed M, Adedotun IO, Olajide M, Irabor CO, Afolabi TI, Gbadebo IO, et al. Virtual screening, ADMET profiling, PASS prediction, and bioactivity studies of potential inhibitory roles of alkaloids, phytosterols, and flavonoids against COVID-19 main protease (Mpro). Nat Prod Res. 2022; 36(12):23 -33.
34. Wongsinlatam W, Remsungnen T. Molecular dynamics simulations of CO2 molecules in ZIF-11 using refined AMBER force field. J Chem. 2013; 1-10.
35. Pabis A, Geronimo I, York DM, Paneth P. Molecular dynamics simulation of nitrobenzene dioxygenase using AMBER force field. J Chem Theory Comput. 2014; 10(6):2246 - 2254.
36. Najib A, Handayani V, Ahmad AR, Hikmat S. Insilico screening chemical compounds α-glucosidase inhibitor from cordia myxa L. Int J Res Pharm Sci. 2019;10(3):1 - 3.
37. Pióro-Jabrucka E, Pawełczak A, Przybył JL, Bączek K, Węglarz Z. Accumulation of phenolic and sterol compounds in Euphorbia hirta (L.). Herba Pol. 2011; 57(2):1-26.
38. Olalere OA, Gan CY. Microwave-assisted extraction of phenolic compounds from Euphorbia hirta leaf and characterization of its morphology and thermal stability. Sep Sci Technol. 2021; 56(11):444-476.
39. Susiloningrum D, Permanasari AA, Adianti M, Tumewu L, Wahyuni TS, Tanjung M, et al. The alkaloid fraction from melicope latifolia leaves inhibits hepatitis C Virus. Pharmacogn J. 2020; 12(3):535 - 540.
40. Gbolade A, Adedokun O, Igbinomwanhia E, Alli M. Lethality of Bryophyllum pinnatum (Lam) Oken (Crassulaceae) Leaf Methanol Extract and Fractions against Naja nigricollis and Bitis arietans Lethality of Bryophyllum pinnatum (Lam .) Oken (Crassulaceae) Leaf Methanol Extract and Fractions against N. 2020;8(July):6–11.
41. Parul R, Kundu SK, Saha P. In Vitro Nitric Oxide Scavenging Activity of Methanol Extracts of Three Bangladeshi Medicinal Plants. Pharma Innov. 2012; 1(12):83–88.
42. Kumar S, Malhotra R, Kumar D. Euphorbia hirta: Its chemistry, traditional and medicinal uses, and pharmacological activities. Vol. 4, Pharmacognosy Reviews. 2010:273-286.
43. Isyaku Y, Uzairu A, Uba S. Computational studies of a series of 2-substituted phenyl-2-oxo-, 2-hydroxyl- and 2-acylloxyethylsulfonamides as potent anti-fungal agents. Heliyon. 2020;6(4): e03724 - 37.
44. Han G, Lee DG. Antibacterial Mode of Action of β-Amyrin Promotes Apoptosis-Like Death in Escherichia coli by Producing Reactive Oxygen Species. J Microbiol Biotechnol. 2022; 28;32(12):1547-1552. doi: 10.4014/jmb.2209.09040.
45. Emmanuel, IA, Olotu F, Agoni, C, Soliman ME, 'Broadening the horizon: Integrative pharmacophore-based and cheminformatics screening of novel chemical modulators of mitochondria ATP synthase towards interventive Alzheimer's disease therapy', Med. Hypotheses 2019; 130:109277. https://doi.org/10.1016/j.mehy.2019.109277
46. Bjij I, Khan S, Betz R, Cherqaoui D, Soliman ME, 'Exploring the structural mechanism of covalently bound E3 ubiquitin ligase: Catalytic or allosteric inhibition?', Protein J. 2018, 37:500–509. https://doi.org/10.1007/ s10930-018-9795-
47. Ndagi U, Mhlongo NN, Soliman ME, 'The impact of Thr91 mutation on c-Src resistance to UM-164: Molecular dynamics study revealed a new opportunity for drug design', Mol. BioSyst. 2017, 13, 1157–1171. https://doi.org/ 10.1039/c6mb00848h
48. Akher FB, Farrokhzadeh A, Olotu FA, Agoni C, Soliman ME, 'The irony of chirality – unveiling the distinct mechanistic binding and activities of 1-(3-(4amino-5-(7-methoxy-5-methylbenzo[b]thiophen2-yl)-7H-pyrrolo[2,3-d]pyrimidin-7-yl)pyrrolidin1-yl)prop-2-en-1-one enantiomers as irreversible covalent FGFR4 inhibitors', Org. Biomol. Chem. 2019; 17:1176–1190. DOI: 10.1039/c8ob02811g
49. Olanlokun JO, Olotu FA, David OM, Idowu TO, Soliman ME, Olorunsogo OO, 'A novel compound purified from Alstonia boonei inhibits Plasmodium falciparum Lactate dehydrogenase and Plasmepsin II', J. Biomol. Struct. Dyn. 2019; 37:2193–2200. DOI: 10.1080/ 07391102.2018.1483840
50. Adewumi AT, Ajadi MB, Soremekun OS, Soliman ME, 'Thompson loop: Opportunities for antitubercular demethylmenaquinone methyltransferase protein', RSC Adv. 2020; 10:23466–23483. https://doi.org/10.1039/ D0RA03206A
51. Adewumi AT, Elrashedy A, Soremekun OS, Ajadi MB, Soliman ME, 'Weak spots inhibition in the Mycobacterium tuberculosis antigen 85 C target for antitubercular drug design through selective irreversible covalent inhibitor-SER124', J. Biomol. Struct. Dyn. 2020. DOI: 10.1080/ 07391102.2020.1844061
52. Kalathiya U, Padariya M, Baginski M, 'Structural, functional, and stability change predictions in human telomerase upon specific point mutations', Sci. Rep. 2019, 9,1–13. https://www.nature.com/articles/s41598-019-45206-y
53. Olotu FA, Soliman ME, 'From mutational inactivation to aberrant gain-of-function: unraveling the structural basis of mutant p53 oncogenic transition', J. Cell. Biochem. 2018; 119: 2646–52. DOI: 10.1002/jcb.26430
54. Adejoro IA, Waheed SO, Adeboye OO, 'Molecular docking studies of Lonchocarpus cyanescens Triterpenoids as Inhibitors for Malaria', J. Phys. Chem. B 2016; 6:1–4. DOI: 10.4172/2161-0398.1000213